Predicting idiopathic toxicity of cisplatin by a pharmacometabonomic approach

Hyuk Nam Kwon[1,6], Mina Kim[2,6], He Wen[1,6], Sunmi Kang[1], Hye-ji Yang[1], Myung-Joo Choi[2], Hee Seung Lee[2], DalWoong Choi[3], In Suh Park[4], Young Ju Suh[5], Soon-Sun Hong[2] and Sunghyouk Park[1]

[1]Department of Biochemistry, Inha University Hospital and Center for Advanced Medical Education by BK21 project, College of Medicine, Inha University, Shinheung-dong 3ga, Chung-gu, Incheon, Korea; [2]Department of Biomedical Sciences, Inha University Hospital and Center for Advanced Medical Education by BK21 project, College of Medicine, Inha University, Shinheung-dong 3ga, Chung-gu, Incheon, Korea; [3]Department of Environmental Health, College of Health Sciences, Korea University, Seoul, Korea; [4]Department of Pathology, Inha University Hospital and Center for Advanced Medical Education by BK21 project, College of Medicine, Inha University, Shinheung-dong 3ga, Chung-gu, Incheon, Korea and [5]Department of Biostatistics, Inha University Hospital and Center for Advanced Medical Education by BK21 project, College of Medicine, Inha University, Shinheung-dong 3ga, Chung-gu, Incheon, Korea

Cisplatin has been one of the most widely used anticancer agents, but its nephrotoxicity remains a dose-limiting complication. Here, we evaluated the idiopathic nature and the predose prediction of cisplatin-induced nephrotoxicity using a nuclear magnetic resonance (NMR)-based pharmacometabonomic approach. Cisplatin produced serious toxic responses in some animals (toxic group), but had little effect in others (nontoxic group), as judged by hematological and histological results. The individual metabolic profiles, assessed by urine NMR spectra, showed large differences between the post-administration profiles of the two groups, indicating the relevance of the NMR approach. Importantly, multivariate analysis of the NMR data showed that the toxic and nontoxic groups can be differentiated based on the pretreatment metabolite profiles. Leave-one-out analysis, performed to evaluate the practical performance of our approach, gave a 66% accuracy rate in predicting toxic responses based on the pretreatment metabolite profiles. Hence, we provide a working model that can explain the idiopathic toxicity mechanism based on marker metabolites found by NMR analysis consistent with tissue NADH measurements. Thus, a pharmacometabonomic approach using pretreatment metabolite profiles may help expedite personalized chemotherapy of anticancer drugs.

Kidney International (2011) **79,** 529–537; doi:10.1038/ki.2010.440; published online 27 October 2010

Correspondence: *Sunghyouk Park, Department of Biochemistry, Inha University Hospital and Center for Advanced Medical Education by BK21 project, College of Medicine, Inha University, Shinheung-dong 3ga, Chung-gu, Incheon, Korea. E-mail: spark@inha.ac.kr or*
Soon-Sun Hong, Department of Biomedical Sciences, Inha University Hospital and Center for Advanced Medical Education by BK21 project, College of Medicine, Inha University, Shinheung-dong 3ga, Chung-gu, Incheon, Korea. E-mail: hongs@inha.ac.kr

[6]These authors contributed equally to this work.

Received 27 May 2010; revised 31 July 2010; accepted 15 September 2010; published online 27 October 2010

KEYWORDS: anticancer; cisplatin; pharmacometabonomics; prediction; toxicity

Cisplatin is a broad spectrum antineoplastic agent used against solid tumors such as ovarian, testicular, bladder, lung, and breast carcinomas.[1–4] Although it has been one of the most widely used chemotherapeutic agents for the last three decades, its nephrotoxicity remains a major concern.[5,6] Cisplatin induces cumulative impairment of renal function manifested by decreased glomerular filtration rate with its major target site being the renal tubule system. As much as 20% of patients on high-dose cisplatin chemotherapy develop severe renal dysfunction.[5,6]

The degree of drug-induced toxic responses varies among patients, and is one of the major factors to determine therapy success and for implementing personalized medicine. However, individualized therapy is still at its incipient stage, and most research has focused on genetic susceptibility based on individual variations in the DNA sequences.[7,8] This pharmacogenomic approach, although useful in some cases,[9] has rather narrow applicability and may not contribute significantly to personalized medicine.[10–12] Pharmacogenomic approaches to anticancer agents have also had modest results, with less-than-expected clinical significance.[13–15]

Pharmacogenomics can only measure innate genetic variability and does not incorporate 'post-birth' environmental and/or personal metabolic factors that could be more important in drug-induced toxic responses. As an alternative, pharmacometabonomics, measuring the final phenotypic effects of both genetic and environmental factors, was recently proposed.[16–19] A pioneering work by Clayton *et al.*[16] showed that the metabolic fate of a drug (paracetamol) and the related toxicity can be predicted based on predose urine metabolite profile from laboratory animals with the same genetic backgrounds. The concept was additionally proven for a different system[18] and, ultimately, for human.[19,20] Other

reports also provided high expectations for its application to personalized drug therapy, disease diagnosis, and pharmaceutical research.[16,20–23] Therefore, pharmacometabonomics is expected to provide holistic understanding of effects of many more drugs and become an important discipline in the practice of medicine.

Anticancer drugs are probably the most appropriate class of drugs, for which the individual toxic responses should be considered. They exhibit toxic responses in larger portions of patients than other classes of drugs and the toxicity is often life threatening or irreversible. The therapeutic indices of these drugs are often quite small and they can exhibit significant toxicity even at recommended therapeutic doses. In addition, the physical condition of cancer patients often may not be adequate for invasive biopsies for toxicity evaluation. Therefore, predicting toxicity before anticancer drug administration using noninvasive pharmacometabonomics is highly desirable. So far, most metabonomics studies on anticancer drugs involve toxicity markers or toxic response assessment after drug administration.[24–26]

Here, we took nuclear magnetic resonance (NMR)-based pharmacometabonomic approach to address the idiopathic nature and the predose prediction of cisplatin-induced nephrotoxicity. We used this particular application of metabonomics, which has been used widely to evaluate kidney function/toxicity in many circumstances.[27–34] Our results show that the animals could be differentiated according to their toxic-response status based on metabolite profiles obtained before cisplatin administration. In addition, these predose urine metabolite profiles could predict the outcomes of the drug toxicity with 66% accuracy rate for the genetically homogenous animals. We also characterized the chemical identities of the contributing metabolites that could predispose the animals to the drug toxicity. These noninvasive approach could be conveniently applied to other anticancer agents and contribute to improving cancer chemotherapy using personal metabolic profiles.

RESULTS

Individual toxic response

We performed preliminary experiments with various doses and administration times of cisplatin in small number of animals (typically $n = 4$–5). During this course, we consistently found that a portion of the tested animals did not show any signs of toxicity at doses, which caused significant damages to others (data not shown). To investigate this individual toxicity difference more systematically, we measured hematological markers for renal toxicity, such as serum blood urea nitrogen (BUN) and creatinine (Cr) level in a larger number of animals ($n = 15$) challenged with a toxic dose (10 mg/kg) of cisplatin (Figure 1a and b). As expected, many of the animals ($n = 10$) developed toxicity, with very high BUN and Cr values. However, as many as five animals showed little difference in these markers from the control

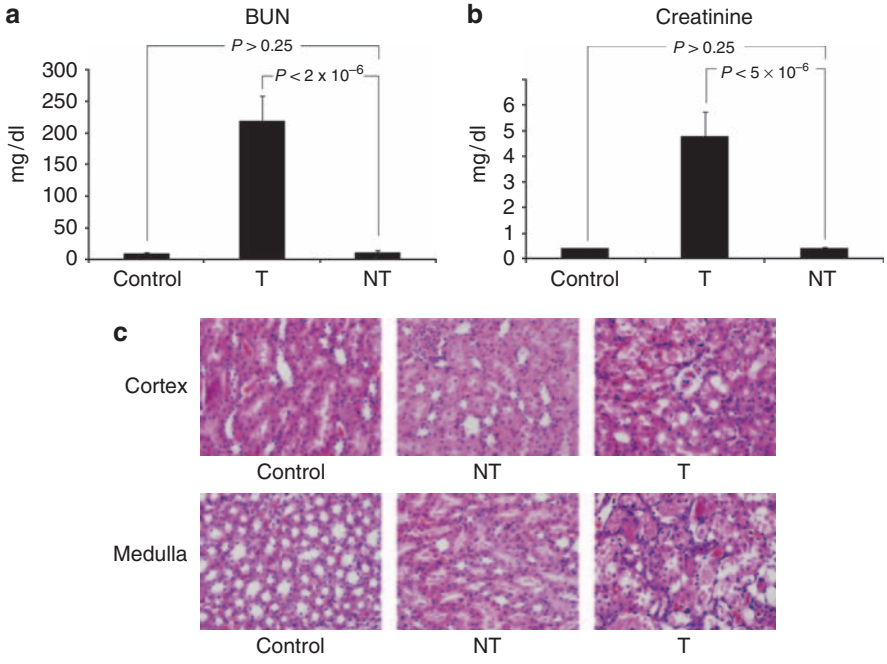

Figure 1 | Individual difference to cisplatin-induced toxicity assessed by hematology markers and histopathology. The control group was given just saline, and the experimental group was given 10 mg/kg of cisplatin in saline. BUN and creatinine levels were measured immediately after killing the animals. The experimental group (total $n = 15$) was divided into two groups, according to the BUN values: NT represents non-toxic group ($n = 5$, BUN < 60) and T represents toxic group ($n = 10$, BUN > 60). (**a**, **b**) Changes in BUN and creatinine levels, respectively. Data are expressed as mean ± s.d. (**c**) Histological evaluation of the cisplatin-induced kidney toxicity. The kidneys were harvested and fixed in 10% formaldehyde. Histological sections of the kidney were stained with H&E. First row is for kidney cortex and second row is for medulla. BUN, blood urea nitrogen; H&E, hematoxylin and eosin.

group. A consistent trend was also observed in body weight changes over a 100-h period (Supplementary Figure S1 online). The differences in the hematology markers were so dramatic (P-values on the order of 10^{-6}, see Figure 1a and b) that we were able to categorize the animals as: non-toxic group (NT-group, $n=5$, BUN <60) and toxic group (T-group, $n=10$, BUN >60). We then evaluated the toxic responses in the individual group in more detail.

As toxicity markers can also be affected by damage to other organs, we performed histopathological studies to confirm direct kidney tissue damage. Hematoxylin and eosin staining of the kidney cortex and medulla showed that the NT-group had mostly intact nuclei and cell shapes, as well as normal tubular and vascular structure, similar to those of the control group (Figure 1c and Supplementary Figure S2 online). In contrast, the T-group showed irregular tubular and cellular structure, suggesting significant damage. Both histopathology and biomarkers confirm that cisplatin can manifest very different individual toxic responses in the kidney.

To ensure that the observed difference in the cisplatin toxicity are not due to different delivery of the drug to kidney in individual animals, the cisplatin levels (as platinum) in the kidney tissues were measured using inductively coupled plasma mass spectrometry technique, one of the best and most sensitive methods to measure heavy metal contents in samples. The measured platinum levels were 22.82 ± 5.70 and 24.18 ± 7.25 (μg/g kidney) for the T- and NT-groups, respectively (Supplementary Figure S3 online). We performed Student's t-test with null hypothesis and obtained P-value of 0.73. These results clearly demonstrate that the kidney platinum levels are not different for the two groups, and that the difference in the cisplatin-induced toxicity does come from the idiopathic responses to the drug. We then tested whether we could differentiate these two groups based on pre-administration metabonomic parameters.

NMR spectral analysis

As all animals have the same genetic background, these idiopathic responses most probably occur from metabolic differences between individuals.[10,16] As pre-administration metabonomic parameters could serve as basis for predicting drug-induced toxicity,[16] we took a metabonomic approach with pre- and post-administration urine. We used urine metabolite profiles measured by H-NMR spectroscopy, as they are exquisitely sensitive to kidney function and metabolic status.[35,36] The post-administration NMR spectra were very different between the T- and NT-groups, with the NT-group similar to the control group (Figure 2, right column). More specifically, the post-administration spectra showed much higher glucose peaks and much lower hippurate, urea, and allantoin peaks in the T-group than the NT-group. This result suggests that cisplatin affects the metabolism of these compounds in the kidney as a result of toxicity. These NMR metabolite profiles are consistent with hematological data, as high BUN indicates low excretion of urea. In addition, the pre-administration profiles of the NT-group were similar to its post-administration profiles, indicating that cisplatin did not affect its kidney metabolism. These results show that metabolic differences can be correlated with differential toxic responses via an NMR-based metabonomic approach.

More appropriate for the pharmacometabonomic prediction of cisplatin toxicity are differences in the pre-administration NMR spectra of T- and NT-groups (Figure 2, left column). Casual examination of the representative spectra did not identify high-intensity peaks whose differences are immediately apparent, which was not surprising considering the homogenous genetic background of the animals. Therefore, we decided to analyze the entire NMR dataset in a more holistic way with multivariate analysis to investigate marker signals with smaller intensities, but high statistical significance for pharmacometabonomic prediction.

Orthogonal projections to latent structure-discriminant analysis (OPLS-DA) multivariate analysis and identification of markers

Our goal was to predict post-administration toxic responses based on the individual differences in the pre-administration metabolic profiles. Therefore, we took multivariate approaches to differentiate the pre-administration urine NMR spectra according to their post-administration responses, that is, T- vs NT-responses. We used OPLS-DA approaches, as it can classify groups in the presence of high structured noise that can otherwise dominate the variations between groups.[37–39] The OPLS-DA model on the NMR metabolite profiles was obtained with one predictive (Pp) and one orthogonal component. Out of the total independent input data, 34.4% were structured and the rest were unstructured noise. Among the structured data, 16.6% was Pp, correlated to the separation of the groups, and 17.8% (Po) was uncorrelated to the separation. The relatively small value of the Pp is not surprising, considering the genetic homogeneity of the animals. It actually shows that the OPLS-DA method can differentiate the groups even in the presence of large amount of other confounding factors. The resulting score plot shows that the T- and NT-groups can be clearly differentiated by the first Pp component derived from the NMR spectral variables (Figure 3).

We also used statistical total correlation spectroscopy[31] analysis to find the contributing signals for this separation (Figure 4). The P(corr)p values of each of these signals suggest that multiple metabolite signals, rather than one overwhelmingly prominent marker, contribute to the differentiation. It is not surprising to see these patterns, as biological responses to drugs often involve multiple molecules. With database matching and analyses of the ultra high-field (900 MHz) two-dimensional NMR spectra, we identified and confirmed 28 metabolites (Supplementary Table S1 online). The representative analyses for two important compounds (see below), oxoglutarate and succinate, are shown in Supplementary Figure S4 online. Among those identified, we picked four metabolites with relatively high Pp and P(corr)p values (1–4 on Figure 4), hence more

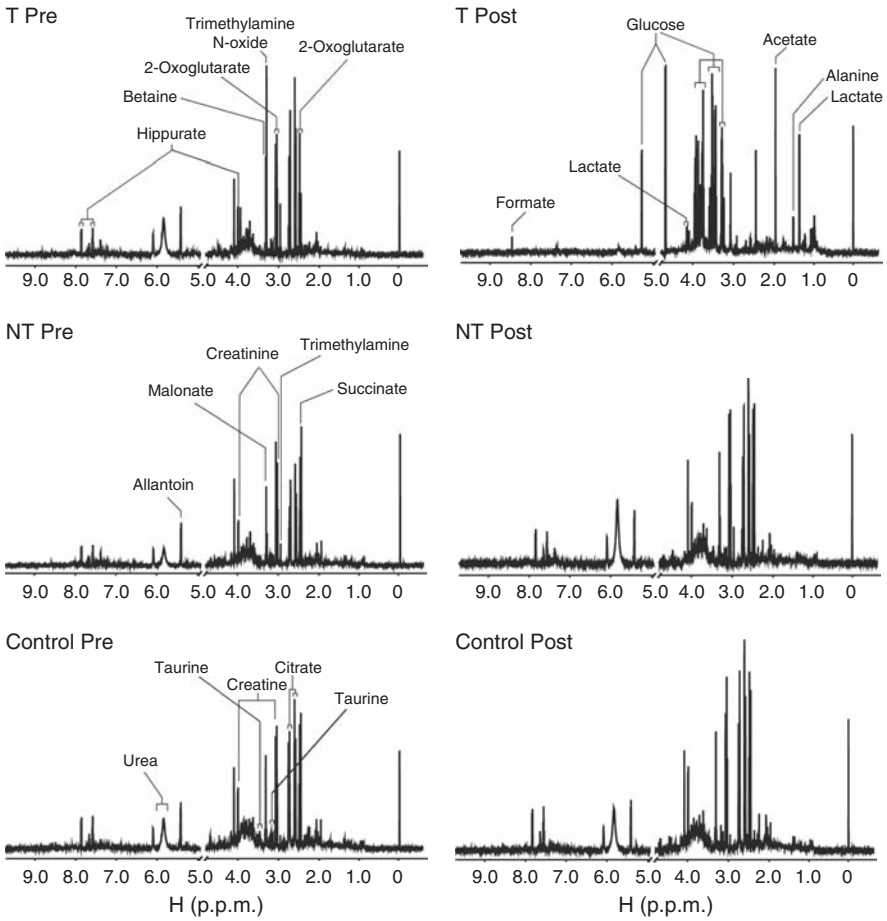

Figure 2 | Representative urine NMR spectra of control, NT-, and T-group at pre- and post-administration points. Spectra for the T-group is in the top, NT-group in the middle, and the control group in the bottom rows. Spectra in the left column are for pre-administration and those in the right for post-administration spectra. Specific metabolite peaks were assigned using Chenomx (Spectral database) and ultra high-field (900 MHz), two-dimensional NMR spectra (see text). The spectra were taken for samples in 500 µl of D_2O and urine mixture containing 200 mmol/l sodium phosphate (pH 7.4) and 0.025% trimethylsilylpropionic acid sodium salt-d_4 as a chemical shift reference. NMR, nuclear magnetic resonance; NT-group, non-toxic group; T-group, toxic group.

relevant to the differentiation, as markers for differentiation of the groups (1: allantoin, 2: creatinine, 3: succinate, 4: oxoglutarate). To confirm the validity of the markers found by this multivariate analysis, we also carried out Mann–Whitney *U*-test.[19] Allantoin, succinate, and Cr levels are statistically higher in the NT-group, whereas oxoglutarate level is higher in the T-group even before cisplatin administration (Supplementary Figure S5 online). We also addressed the biological and statistical significance of these markers by measuring the nicotinamide adenine dinucleotide (NADH) levels in kidney tissues (see the Discussion section) and performing false discovery rate and Bonferroni analysis (Supplementary Table S2 online). Our data confirm that metabolic differences exist in these animals despite the identical genetic backgrounds and that NMR-based metabonomics approach can characterize the markers responsible for the idiopathic toxic responses.

Prediction of toxicity

With the successful pre-administration distinction between the T- and NT-groups, we further validated the approach by performing a leave-one-out analysis on the OPLS-DA model. Although not usually performed in the metabonomics literature, this is an important step to evaluate the practical quantitative performance of the approach. We left out one sample at a time and predicted the toxicity from the model established with the rest of the dataset. This approach, therefore, serves as a blind test for an unknown sample and provides real-life cross-validation for the established model. Our OPLS-DA model could correctly classify the unknown samples with 66% accuracy rate for toxicity response (Figure 5).

DISCUSSION

Cisplatin, along with other related 'platins', is an important anticancer agent with broad indications in solid tumor chemotherapy.[40–42] However, its prominent nephrotoxicity often leads to treatment cessation.[5] There has been much research on how to evaluate or reduce its kidney toxicity during or after the treatment.[5,40,43,44] However, most relevant for cisplatin toxicity evaluation would be to predict its toxic responses at the individual level before administration, but

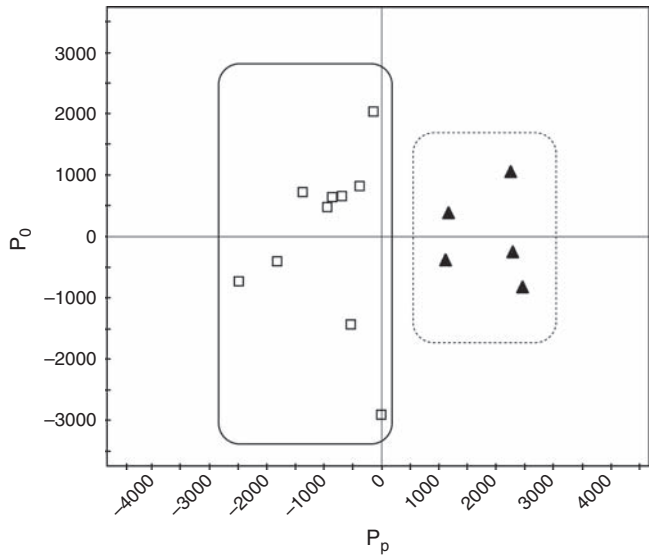

Figure 3 | Differentiation of T- and NT-groups based on pre-administration metabonomic profiles. Orthogonal projections to latent structure-discriminant analysis (OPLS-DA) score plot of the toxic and non-toxic group. Open box, T-group samples; filled triangle, NT-group samples. The model was established using one predictive and one orthogonal component. NT-group, non-toxic group; Pp, predictive; T-group, toxic group.

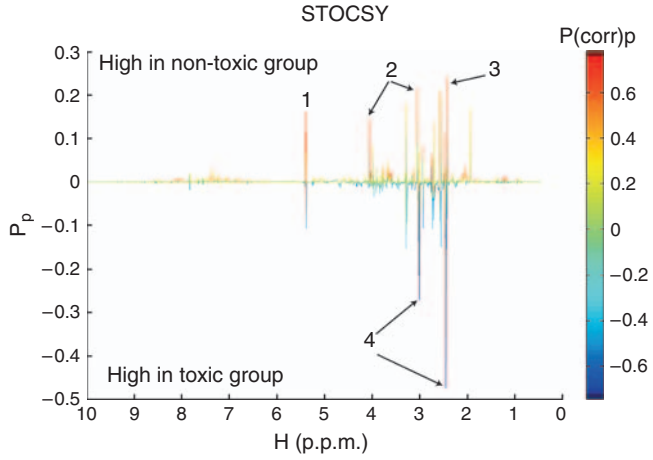

Figure 4 | Variable contributions from 1D projection of the statistical total correlation spectroscopy (STOCSY). The Pp represents modeled covariation and P(corr)p represents modeled correlation, which is shown in the color scale on the right. Prominent signals for metabolites that are unequally distributed between the T- and NT-groups are indicated with numbers (1: allantoin, 2: creatinine, 3: succinate, 4: oxoglutarate). NT-group, non-toxic group; Pp, predictive; T-group, toxic group.

little has been reported on this. Here, we applied the NMR-based pharmacometabonomic approach to cisplatin-associated kidney toxicity, and were able to predict individual toxicity with predose metabolic profiles. In addition, our data showed that some metabolite levels are quite different among individuals, suggesting idiopathic metabolic differences even for genetically homogenous animals.

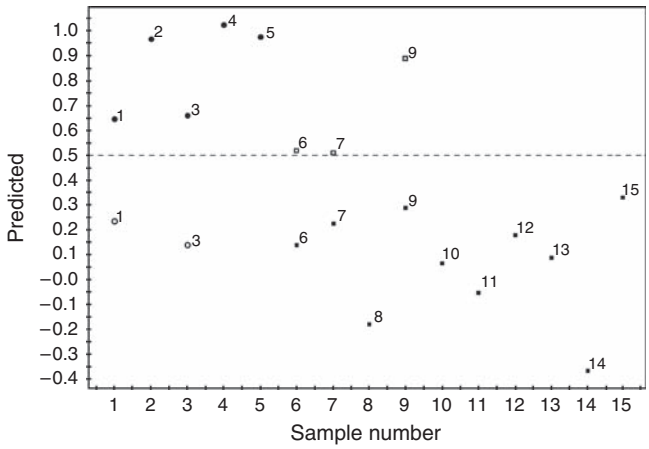

Figure 5 | Prediction of idiopathic toxic responses for unknown samples. Prediction was performed based on the OPLS-DA model using leave-one-out analysis. One sample (unknown) was left out at a time and toxicity was predicted until all the samples were left out once. The class membership of the left-out samples was predicted using an *a priori* cutoff value of 0.5 (dashed line).[62] NT-group, filled circle; T-group, filled box. The *y* axis values of the filled symbols are from the analysis using the entire data set. In the case of misclassified samples, the predicted *y* axis values from the leave-one-out analysis are also shown as open boxes (T-group) and open circles (NT-group). NT-group, non-toxic group; OPLS-DA, orthogonal projections to latent structure-discriminant analysis; T-group, toxic group.

Among the differential metabolites, oxoglutarate is a key intermediate in oxygen-consuming metabolism through the tricarboxylic acid cycle. It is converted to succinate by oxoglutarate dehydrogenase followed by succinyl-CoA synthetase, with concomittent generation of NADH. The higher and lower levels of oxoglutarate and succinate, respectively, in the pre-administration samples of the T-group suggest that the flux through this metabolic step in the tricarboxylic acid cycle might be less efficient in that group, which could lead to inefficient production of NADH. To test this hypothesis directly, we measured the NADH levels in kidney tissues using an enzymatic assay (Figure 6). The result confirms that the NADH level is significantly lower in the T-group than NT-group. In addition, the values were not appreciably different between the NT and control groups. These metabolic differences between the T- and NT-groups can produce very different outcomes when high reducing power is needed with the drug challenge, even though they may not elicit clear phenotypic differences under normal physiological conditions. It is due to the fact that NADH is important in providing a reservoir of reducing power[45,46] with its quantitative conversion to NADPH by nicotinamide nucleotide transhydrogenase.[47] In turn, NADPH is consumed in the detoxification of reactive oxygen species (ROS) by glutathione reductase (Figure 7). NADH can also act more directly as a reducing agent in repairing disulfide-oxidized proteins through protein disulfide reductase.

As the main mechanism of cisplatin toxicity is the generation of ROS,[5,43] the above metabolic difference might

be a risk factor for increased cisplatin toxicity. The T-group, with the less efficient conversion of oxoglutarate to succinate, may not produce enough NADH to help detoxify the ROS produced by cisplatin, leading to the accumulation of ROS-mediated cellular damages. The approximately twofold difference in the oxoglutarate–succinate levels might be amplified into much larger differences in kidney damages, as oxidative damage is cumulative. The metabolic difference can also be amplified in the detoxification enzyme chain reactions that deliver the reduction potential to ROS (Figure 7). We believe our biological data for NADH levels and statistical analysis with false discovery rate and Bonferroni adjustment (Supplementary Table S2 online) give strong enough support for the significance of the marker metabolites.

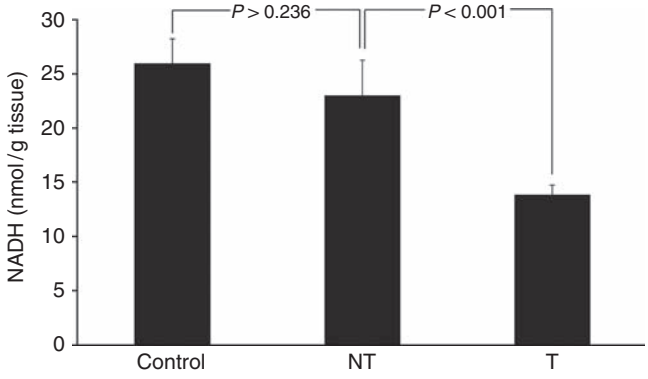

Figure 6 | NADH levels in the kidney tissues. The NADH levels were measured using the NAD/NADH measuring kit from Abcam following the manufacturer's instruction. Kidney tissues were obtained after killing of the animals following the drug treatment. The NT- and T-groups were divided according to the BUN values after the cisplatin treatment: the NT-group with BUN <60 and the T-group with BUN >60. The control group was given only vehicle. Data are expressed as mean $\pm$ s.d. *P*-values from student's *t*-test are also shown. BUN, blood urea nitrogen; NADH, nicotinamide adenine dinucleotide; NT-group, non-toxic group; T-group, toxic group.

The levels of allantoin and Cr in the NT group, as estimated by NMR, were also significantly different from that in the T group (Supplementary Figure S5 online). The median levels of both molecules were about 1.4 times larger in the NT group. It is interesting to note that both Cr and allantoin are terminal metabolites eliminated by kidney. Allantoin is produced from catabolism of purines, and Cr is produced from creatine phosphate. The levels of these molecules, especially Cr, have been shown to correlate with general kidney functions. Allantoin was also proposed as a kidney functional marker in reperfusion injury[35] or renal failure cases.[48] Therefore, the levels of these molecules might represent general capacity of the kidney function and metabolism, which, in turn, might partially contribute to the toxicity differences between the T- and NT-groups. As in the oxoglutarate and succinate cases, although the relatively small differences in the levels of these metabolites between the T- and NT-groups may be irrelevant in physiological conditions, the cumulative nature of ROS-mediated cisplatin toxicity may result in large differences in the final manifestation of tissue damages by the drug.

Predicting toxic responses before drug administration constitutes an important part of personalized drug therapy, and is especially important for drugs those toxicities are serious and irreversible, such as anticancer agents. Although pharmacogenomic approaches have been tested widely for anticancer drugs, actual clinical application is limited to handful of cases, such as imatinib, trastuzumab, Erlotinib, and other closely related drugs.[49–51] In addition, the indications of these drugs are quite limited, because they are target-selective narrow spectrum agents. Pharmacogenomic approaches have been possible for these drugs, because their target proteins, such as epidermal growth factor receptor or BCR-ABL kinase, are exactly known before the drug development. In comparison, the pharmacometabonomic approach is applicable to anticancer agents with wider spectrum without previous knowledge about the targets, because it detects more systemic variation using biofluids. Our results indicate that the pharmacometabonomic

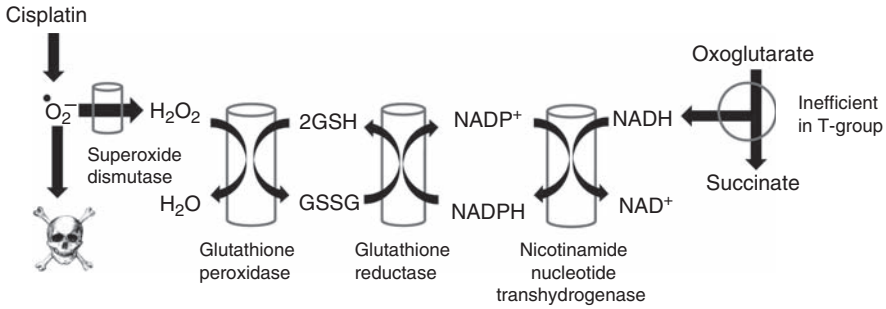

Figure 7 | Molecular events linking the pre-administration metabonomic difference to the idiopathic cisplatin toxicity. The T-group has lower efficiency of the oxoglutarate to succinate conversion step in the TCA cycle, which should result in lower levels of NADH. Although this difference may not exhibit any noticeable difference under physiological conditions, cisplatin challenges can make a difference. In the T-group, less NADH will result in less efficient disposal of ROS generated by cisplatin because of the metabolic linkage between ROS detoxification (glutathione peroxidase) and NADH. Cumulative differences in this detoxification efficiency could produce idiopathic toxic responses to cisplatin. NADH, nicotinamide adenine dinucleotide; ROS, reactive oxygen species; T-group, toxic group; TCA, tricarboxylic acid cycle.

approach may find broad application in anticancer agents where the pharmacogenomic approach was not satisfactory. Cisplatin is an appropriate test case for pharmacometabonomic approach for anticancer agents, as it is one of the most widely used broad-spectrum agents without narrowly defined targets. In addition, it induces irreversible kidney damages in a significant portion of the patients.[5,6]

Just like other biomarkers, the accuracy rate for the prediction of the current metabonomics approach for cisplatin is not perfect. It is still very meaningful considering that clinical markers for early cancer diagnosis have low to modest sensitivities: cancer antigen 27.29 with 30% for early breast cancer,[52] carcinoembryonic antigen with 25% for early colon cancer,[53] and prostate specific antigen with 75% for organ-confined prostate cancer.[54] Although the current study does not involve a very large number of animals, our data suggest that, with a properly built database of urine NMR spectra, a toxic response can be predicted before cisplatin administration with quantitative assessment of prediction accuracy. Future research on the prediction of efficacy, which may also be addressed using metabonomics, can be combined with the current approach to help achieve the ultimate goal of personalized cisplatin treatment.

METHODS

Reagents and animals

Cisplatin (CAS no. 15663-27-1; lot 059H3657) was purchased from Sigma Chemical Company (St Louis, MO). Male Sprague–Dawley rats (200 g, 6–7 weeks of age) were purchased from Orient Bio (Sungnam, Korea) and housed on 12 h light/dark cycle before the experiment. The animals were fed cereal-based standard chow with free access to water. Animal care and all experimental procedures were conducted in accordance with the guide for animal experiments edited by the Korea Academy of Medical Science, Declaration of Helisinki principle, and approved by the institutional review board.

Administration of cisplatin and sampling

Rats were divided into two treatment groups, and all injections were given intraperitoneally. The control group ($n = 4$) was given just saline, and the cisplatin treated group ($n = 15$) was given 10 mg/kg of cisplatin in saline. Individual predose (−24–0 h) and postdose (72–96 h) urine samples were collected into an ice-cooled jar with a metabolic cage. Sodium azide was added in the urine collection bowl (0.5 ml of 100 mg/ml solution) to prevent bacterial growth. The pooled urine samples were frozen and stored at −80 °C for subsequent analysis. All animal experiments were done at the Inha University Medical School Animal Experiment Center (Incheon, Korea). Individual animal data are listed in Supplementary Table S3 online.

Hematology markers, histological study, and biochemical NADH assay

After the postdose urine collection, animals were killed and the blood was obtained for clinical chemistry (BUN and Cr levels). The kidneys were harvested and fixed in 10% formaldehyde. Histological sections of the kidney were stained with hematoxylin and eosin stains. NADH level was measured using a NAD/NADH assay kit from Abcam following the vendor-provided instructions (Cambridge, MA). Statistical analysis was performed using an unpaired Student's *t*-test on SPSS software for Windows (Version 10.0; SPSS, Chicago, IL).

NMR measurement

All one-dimensional NMR spectra of the urine samples were measured with an NMR spectrometer (Bruker Biospin, Rheinstetten, Germany, Avance 500) operating at a proton NMR frequency of 500.13 MHz. The acquisition parameters were essentially the same as previously reported.[37,55,56] For structural analysis of the metabolites, ultra high field, two-dimensional NMR spectra were acquired using a 900 MHz Bruker Avance spectrometer equipped with a cryogenic probe. For proton correlations, double quantum filtered correlation spectroscopy data were obtained in phase sensitive mode. The data set comprises 1024×192 complex points for the direct and indirect dimensions, respectively. For proton and carbon long-range correlation, a heteronuclear multiple-bond correlation spectrum was measured in magnitude mode. The dataset comprises 1024 complex points for direct and 512 real points for indirect dimension. The one-bond proton carbon correlation was measured with a heteronuclear single-quantum coherence spectrum. The dataset comprises 1024×192 complex points for the direct and indirect dimensions, respectively. The spectra were referenced against the trimethylsilylpropionic acid sodium salt-d_4 signal. All datasets were processed with nmrPipe software (NMR Science, North Potomac, MD) and analyzed with nmrView software (One Moon Scientific, Westfield, NJ). We also used Chenomx (Spectral database; Edmonton, Canada) for identification of the metabolites. This study used the NMR facility at Korea Basic Science Institute, which is supported by Bio-MR Research Program of the Korean Ministry of Science and Technology (E29070).

Determination of cisplatin levels in kidney

To analyze the cisplatin concentrations in kidney, the frozen kidney samples were pretreated with microwaves. Kidney samples (0.5 gram) were put into a Teflon vessel to which 70% nitric acid (5 ml) and distilled deionized water (5 ml) were added. After closing the top, the samples were decomposed with the microwave digestion system (Ethos, Millestone, Italy). For the decomposition, the temperature was increased to 180 °C for 15 min in the first step and the temperature was maintained at 180 °C for 15 min in the second step. In the third step, the vessel was cooled down to room temperature for 120 min. The pretreated samples were diluted with distilled deionized water. Platinum analysis was carried out with an induced coupled plasma-mass spectrometer (7500 series, Agilent, Santa Clara, CA). The cisplatin levels were expressed as platinum concentrations in the kidney samples.

Multivariate data analysis

All the obtained time domain NMR data were Fourier transformed, phase corrected, and baseline corrected manually. The resulting frequency domain data were binned at a 0.0044 p.p.m. interval to reduce the complexity of the NMR data for pattern recognition. The high-resolution binned data were aligned using a correlation-optimized warping algorithm.[57] The signals were normalized against total integration values, 0.025% trimethylsilylpropionic acid sodium salt-d_4, and then converted to an ascii text file for the next step. The binning, normalization, and conversion were done using in-house written Perl software. For statistical analysis, water and urea regions were excluded. Multivariate statistical analysis was performed using

numeric data processing software: Matlab (MathWorks, Natick, MA), SIMCA-P version 11.0 (Umetrics, Umeå, Sweden). OPLS-DA was performed with one Pp and one orthogonal component.[39,58] 1D projection of statistical total correlation spectroscopy was built by overlaying the color-coded correlation values on to the OPLS-DA variable plot.[31,59–61] Prediction of the unknown samples was performed by leave-one-out analysis. One sample (unknown) was left out at a time and the OPLS-DA prediction model was obtained until all the samples were left out once. The class membership of the left-out samples was predicted using an *a priori* cutoff value of 0.5.[62]

DISCLOSURE

All the authors declared no competing interests.

ACKNOWLEDGMENTS

This work was supported by grants from the Korea Healthcare technology R&D Project, Ministry for Health, Welfare and Family Affairs, Republic of Korea (A084338) and (A092006).

SUPPLEMENTARY MATERIAL

Table S1. Assignments of metabolite chemical shifts using Chenomx database and analyses of 900 MHz two-dimensional NMR spectra.
Table S2. False discovery rate (FDR) and Bonferroni analysis for the four marker metabolites.
Table S3. Individual body weight, BUN, and creatinine.
Figure S1. Body weight measurement as a function of time.
Figure S2. Other medullary sections for control and NT groups.
Figure S3. Cisplatin levels in the kidney tissues measured as platinum concentration with inductively coupled plasma mass spectroscopy.
Figure S4. Chemical structure elucidation of contributing signals.
Figure S5. Mann–Whitney *U*-test for the marker signals identified by STOCSY.
Supplementary material is linked to the online version of the paper at http://www.nature.com/ki

REFERENCES

1. Muggia F. Platinum compounds 30 years after the introduction of cisplatin: implications for the treatment of ovarian cancer. *Gynecol Oncol* 2009; **112**: 275–281.
2. Boulikas T, Vougiouka M. Recent clinical trials using cisplatin, carboplatin and their combination chemotherapy drugs (review). *Oncol Rep* 2004; **11**: 559–595.
3. Smith IE, Talbot DC. Cisplatin and its analogues in the treatment of advanced breast cancer: a review. *Br J Cancer* 1992; **65**: 787–793.
4. Crino L, Calandri C, Maestri A *et al.* Gemcitabine and cisplatin combination in early-stage non-small-cell lung cancer. *Oncology (Williston Park)* 2001; **15**: 40–42.
5. Yao X, Panichpisal K, Kurtzman N *et al.* Cisplatin nephrotoxicity: a review. *Am J Med Sci* 2007; **334**: 115–124.
6. Arany I, Safirstein RL. Cisplatin nephrotoxicity. *Semin Nephrol* 2003; **23**: 460–464.
7. Vizirianakis IS. Improving pharmacotherapy outcomes by pharmacogenomics: from expectation to reality? *Pharmacogenomics* 2005; **6**: 701–711.
8. Mancinelli L, Cronin M, Sadee W. Pharmacogenomics: the promise of personalized medicine. *AAPS J* 2002; **2**: 29-41.
9. Furuta T, Sugimoto M, Shirai N *et al.* CYP2C19 pharmacogenomics associated with therapy of Helicobacter pylori infection and gastro-esophageal reflux diseases with a proton pump inhibitor. *Pharmacogenomics* 2007; **8**: 1199–1210.
10. Nebert DW, Jorge-Nebert L, Vesell ES. Pharmacogenomics and 'individualized drug therapy': high expectations and disappointing achievements. *Am J Pharmacogenomics* 2003; **3**: 361–370.
11. Arnett DK, Claas SA, Lynch AI. Has pharmacogenetics brought us closer to 'personalized medicine'for initial drug treatment of hypertension? *Curr Opin Cardiol* 2009; **24**: 333.
12. Ikediobi ON, Shin J, Nussbaum RL *et al.* Addressing the challenges of the clinical application of pharmacogenetic testing. *Clin Pharmacol Ther* 2009; **86**: 28–31.
13. Oldenburg J, Fossa SD, Ikdahl T. Genetic variants associated with cisplatin-induced ototoxicity. *Pharmacogenomics* 2008; **9**: 1521–1530.
14. Huang RS, Duan S, Shukla SJ *et al.* Identification of genetic variants contributing to cisplatin-induced cytotoxicity by use of a genomewide approach. *Am J Hum Genet* 2007; **81**: 427–437.
15. Dawood S, Leyland-Jones B. Pharmacology and pharmacogenetics of chemotherapeutic agents. *Cancer Invest* 2009; **27**: 482–488.
16. Clayton TA, Lindon JC, Cloarec O *et al.* Pharmaco-metabonomic phenotyping and personalized drug treatment. *Nature* 2006; **440**: 1073–1077.
17. Schnackenberg LK. Global metabolic profiling and its role in systems biology to advance personalized medicine in the 21st century. *Expert Rev Mol Diagn* 2007; **7**: 247–259.
18. Li H, Ni Y, Su M *et al.* Pharmacometabonomic phenotyping reveals different responses to xenobiotic intervention in rats. *J Proteome Res* 2007; **6**: 1364–1370.
19. Clayton TA, Baker D, Lindon JC *et al.* Pharmacometabonomic identification of a significant host-microbiome metabolic interaction affecting human drug metabolism. *Proc Natl Acad Sci USA* 2009; **106**: 14728–14733.
20. Wilson ID. Drugs, bugs, and personalized medicine: pharmacometabonomics enters the ring. *Proc Natl Acad Sci USA* 2009; **106**: 14187–14188.
21. Nebert DW, Vesell ES. Can personalized drug therapy be achieved? A closer look at pharmaco-metabonomics. *Trends Pharmacol Sci* 2006; **27**: 580–586.
22. Ala-Korpela M. Potential role of body fluid 1H NMR metabonomics as a prognostic and diagnostic tool. *Expert Rev Mol Diagn* 2007; **7**: 761–773.
23. Lindon JC, Holmes E, Nicholson JK. Metabonomics techniques and applications to pharmaceutical research & development. *Pharm Res* 2006; **23**: 1075–1088.
24. Wang EJ, Snyder RD, Fielden MR *et al.* Validation of putative genomic biomarkers of nephrotoxicity in rats. *Toxicology* 2008; **246**: 91–100.
25. Portilla D, Li S, Nagothu KK *et al.* Metabolomic study of cisplatin-induced nephrotoxicity. *Kidney Int* 2006; **69**: 2194–2204.
26. Morvan D, Demidem A. Metabolomics by proton nuclear magnetic resonance spectroscopy of the response to chloroethylnitrosourea reveals drug efficacy and tumor adaptive metabolic pathways. *Cancer Res* 2007; **67**: 2150–2159.
27. Kim K, Aronov P, Zakharkin SO *et al.* Urine metabolomic analysis for kidney cancer detection and biomarker discovery. *Mol Cell Proteomics* 2009; **8**: 558–570.
28. Nicholson JK, Connelly J, Lindon JC *et al.* Metabonomics: a platform for studying drug toxicity and gene function. *Nat Rev Drug Discov* 2002; **1**: 153–161.
29. Niemann CU, Serkova NJ. Biochemical mechanisms of nephrotoxicity: application for metabolomics. *Expert Opin Drug Metab Toxicol* 2007; **3**: 527–544.
30. Wishart DS. Metabolomics in monitoring kidney transplants. *Curr Opin Nephrol Hypertens* 2006; **15**: 637–642.
31. Cloarec O, Dumas ME, Craig A *et al.* Statistical total correlation spectroscopy: an exploratory approach for latent biomarker identification from metabolic 1H NMR data sets. *Anal Chem* 2005; **77**: 1282–1289.
32. Beger RD, Sun J, Schnackenberg LK. Metabolomics approaches for discovering biomarkers of drug-induced hepatotoxicity and nephrotoxicity. *Toxicol Appl Pharmacol* 2010; **243**: 154–166.
33. Sieber M, Hoffmann D, Adler M *et al.* Comparative analysis of novel noninvasive renal biomarkers and metabonomic changes in a rat model of gentamicin nephrotoxicity. *Toxicol Sci* 2009; **109**: 336–349.
34. Xie G, Zheng X, Qi X *et al.* Metabonomic evaluation of melamine-induced acute renal toxicity in rats. *J Proteome Res* 2010; **9**: 125–133.
35. Serkova N, Fuller TF, Klawitter J *et al.* H-NMR-based metabolic signatures of mild and severe ischemia/reperfusion injury in rat kidney transplants. *Kidney Int* 2005; **67**: 1142–1151.
36. Wei L, Liao P, Wu H *et al.* Metabolic profiling studies on the toxicological effects of realgar in rats by (1)H NMR spectroscopy. *Toxicol Appl Pharmacol* 2009; **234**: 314–325.
37. Kang J, Choi MY, Kang S *et al.* Application of a 1H nuclear magnetic resonance (NMR) metabolomics approach combined with orthogonal projections to latent structure-discriminant analysis as an efficient tool for discriminating between Korean and Chinese herbal medicines. *J Agric Food Chem* 2008; **56**: 11589–11595.

38. Wiklund S, Johansson E, Sjostrom L *et al.* Visualization of GC/TOF-MS-based metabolomics data for identification of biochemically interesting compounds using OPLS class models. *Anal Chem* 2008; **80**: 115–122.
39. Trygg J, Wold S. Orthogonal projections to latent structures (O-PLS). *J Chemom* 2002; **16**: 119–128.
40. Wang D, Lippard SJ. Cellular processing of platinum anticancer drugs. *Nat Rev Drug Discov* 2005; **4**: 307–320.
41. Siddik ZH. Cisplatin: mode of cytotoxic action and molecular basis of resistance. *Oncogene* 2003; **22**: 7265–7279.
42. Cohen SM, Lippard SJ. Cisplatin: from DNA damage to cancer chemotherapy. *Prog Nucleic Acid Res Mol Biol* 2001; **67**: 93–130.
43. Santos NAG, Cat o CS, Martins NM *et al.* Cisplatin-induced nephrotoxicity is associated with oxidative stress, redox state unbalance, impairment of energetic metabolism and apoptosis in rat kidney mitochondria. *Arch toxicol* 2007; **81**: 495–504.
44. Pabla N, Dong Z. Cisplatin nephrotoxicity: mechanisms and renoprotective strategies. *Kidney Int* 2008; **73**: 994–1007.
45. Bellomo G, Martino A, Richelmi P *et al.* Pyridine-nucleotide oxidation, Ca2+ cycling and membrane damage during tert-butyl hydroperoxide metabolism by rat-liver mitochondria. *Eur J Biochem* 1984; **140**: 1–6.
46. Jocelyn PC. The reduction of diamide by rat liver mitochondria and the role of glutathione. *Biochem J* 1978; **176**: 649–664.
47. Hoek JB, Rydstrom J. Physiological roles of nicotinamide nucleotide transhydrogenase. *Biochem J* 1988; **254**: 1–10.
48. Kand'ar R, Zakova P. Allantoin as a marker of oxidative stress in human erythrocytes. *Clin Chem Lab Med* 2008; **46**: 1270–1274.
49. Jiang G, Yang F, Li M *et al.* Imatinib (ST1571) provides only limited selectivity for CML cells and treatment might be complicated by silent BCR-ABL genes. *Cancer Biol Ther* 2003; **2**: 103–108.
50. Reddy GK. Relevance of epidermal growth factor receptor genomic gain in predicting clinical response to kinase inhibitors in non-small-cell lung cancer. *Clin Lung Cancer* 2005; **7**: 163–165.
51. Nakeeb A, Pitt HA, Sohn TA *et al.* Cholangiocarcinoma. A spectrum of intrahepatic, perihilar, and distal tumors. *Ann Surg* 1996; **224**: 463–473; discussion 473–475.
52. Gion M, Mione R, Leon AE *et al.* Comparison of the diagnostic accuracy of CA27.29 and CA15.3 in primary breast cancer. *Clin Chem* 1999; **45**: 630–637.
53. Bast Jr RC, Ravdin P, Hayes DF *et al.* 2000 Update of recommendations for the use of tumor markers in breast and colorectal cancer: clinical practice guidelines of the American Society of Clinical Oncology. *J Clin Oncol* 2001; **19**: 1865–1878.
54. Pound CR, Partin AW, Eisenberger MA *et al.* Natural history of progression after PSA elevation following radical prostatectomy. *JAMA* 1999; **281**: 1591–1597.
55. Kang J, Lee S, Kang S *et al.* NMR-based metabolomics approach for the differentiation of ginseng (Panax ginseng) roots from different origins. *Arch Pharm Res* 2008; **31**: 330–336.
56. Wen H, Yoo SS, Kang J *et al.* A new NMR-based metabolomics approach for the diagnosis of biliary tract cancer. *J Hepatol* 2010; **52**: 228–233.
57. Tomasi G, van den Berg F, Andersson C. Correlation optimized warping and dynamic time warping as preprocessing methods for chromatographic data. *J Chemometr* 2004; **18**: 231–241.
58. Bylesjo M, Rantalainen M, Cloarec O *et al.* OPLS discriminant analysis: combining the strengths of PLS-DA and SIMCA classification. *J Chemom* 2006; **20**: 341–351.
59. Couto Alves A, Rantalainen M, Holmes E *et al.* Analytic properties of statistical total correlation spectroscopy based information recovery in (1)H NMR metabolic data sets. *Anal Chem* 2009; **81**: 2075–2084.
60. Sands CJ, Coen M, Maher AD *et al.* Statistical total correlation spectroscopy editing of 1H NMR spectra of biofluids: application to drug metabolite profile identification and enhanced information recovery. *Anal Chem* 2009; **81**: 6458–6466.
61. Maher AD, Cloarec O, Patki P *et al.* Dynamic biochemical information recovery in spontaneous human seminal fluid reactions via 1H NMR kinetic statistical total correlation spectroscopy. *Anal Chem* 2009; **81**: 288–295.
62. Brindle JT, Antti H, Holmes E *et al.* Rapid and noninvasive diagnosis of the presence and severity of coronary heart disease using 1H-NMR-based metabonomics. *Nat Med* 2002; **8**: 1439–1444.